

Development of Resin Coated Piston suitable for Monolithic Cylinders made of Hypereutectic Al-Si Alloy

Keita Watanabe Hiroataka Kurita

当論文は、JSAE 20229010/SAE 2022-32-0010として、SETC2022 (Small Powertrains and Energy Systems Technology Conference)にて発表されたものです。

Reprinted with permission Copyright © 2022 SAE Japan and Copyright © 2022 SAE INTERNATIONAL
(Further use or distribution is not permitted without permission from SAE.)

要旨

DiASil[®] シリンダに適合すべく、より高い耐久性を有する樹脂コートピストンを開発した。樹脂材料は従来よりも低温で架橋が促進されるよう改良され、ピストンの過時効を抑制しつつ、摩擦摩耗特性を改善した。またピストンスカート上に深い条痕形状を与えることで、シリンダとの焼付きを大幅に遅延させた。最後に、焼付きへの影響因子と深条痕の樹脂コート印刷性について考察した。

Abstract

This study focuses on improving durability of the resin coated piston developed especially for the monolithic cylinder made of a hypereutectic Al-Si alloy, so-called DiASil[®]. The newly developed resin was designed to be cured at a relatively low temperature considering over-aging of a piston and confirmed that it exhibited a lower friction coefficient compared to an existing resin coating. Furthermore, pistons of which skirts had various depth and pitch of grooves filled with the resin coating were offered to evaluate wear and seizure characteristics. The results showed deeper grooves on piston skirts were remarkably effective to delay a seizure. All the seizures were triggered when the ratio of Al substrate exposed to the sliding surface reached up to 60-80%, which implied it can be the empirical criteria for a seizure. Therefore, it can be considered the seizure does not occur as long as adequate resin coating remained in the grooves. Finally, influential factors for the seizure and printability of deep grooves were discussed.

1

INTRODUCTION

In recent years, growing environmental concerns have encouraged the automotive industry to develop an engine with superior fuel economy. Reducing friction losses is recognized one of effective approaches to save energy. Especially, the friction loss derived from sliding resistance between a piston equipped with piston rings and a cylinder bore has attracted great attention since it is considered 45% of friction losses among all the engine components is attributed to the piston assembly^[1]. By covering piston skirts with a resin material including solid lubricants, the friction loss between the piston and the cylinder can be reduced, so the resin coating technology has been widely used in the automotive sector.

A monolithic cylinder, so-called DiASil[®] (hereafter DiASil), is made of a hypereutectic Al-Si alloy so that primary Si particles with high hardness can appear on the cylinder bore surface^[2]. Those particles play a key role to improve resistance against wear and seizure without a cast iron sleeve^[3]. Owing to the sleeveless design, it can realize excellent heat dissipation and lightweight. On the other hands, DiASil cylinder has made it difficult to utilize a resin coated piston because conventional resin coatings can be easily worn out in short term by sliding against the bore surface exposing hard Si particles. Dissipation of the resin coating incurs not only deterioration of fuel efficiency but also a risk of the seizure between the piston skirt and the cylinder bore at the worst case. Therefore, hard Fe plating instead of resin coating have

been used on the piston skirt mating with DiASil cylinder so far.

From this kind of backgrounds, the authors developed a resin coated piston suitable for DiASil cylinder in the previous work^[4]. The piston skirts were coated with a polyamide imide resin including newly blended solid lubricants and hard fillers to achieve a good balance between low friction and high anti-wear property. Additionally, uniform coating thickness up to 20 μ m was enabled in a single screen-printing process so as to extend the coating lifetime. However, higher durability of the resin coated piston is still required because the sliding condition between the piston skirt and the cylinder bore has been increasingly becoming more severe due to recent engine features such as a high compression ratio and a low viscosity oil. Thus, this study is aimed to improve durability of the resin coated piston furthermore by means of novel approaches focusing on cross-linked structures in the resin material and a geometry of the piston skirt surface.

2 EXPERIMENTAL

2-1. Cross-linked structure firmness of new resin

The coating material developed in the previous report^[4] was mainly composed of solid lubricants, hard fillers, polyamide imide as a binder and N-methyl-2-pyrrolidone as a solvent, which is hereafter referred to as “existing material”. Polyamide imide is one of super engineering plastics and well known as a preferable coating material for the piston skirt. Although it is recommended to be cured at 230°C or above, curing at a lower temperature is likely to be carried out in a practical process since higher temperature over 200°C may cause undesirable over-aging of the piston alloy. Curing at lower temperature results in incomplete cross-linked structures of polyamide imide, which will prevent it from fully demonstrating the potential. To clear way for this problem, a new resin has been modified to be cured completely at a temperature lower than that in the piston aging process. This new material with modified resin is hereafter called as “modified material”.

Firstly, a test to evaluate firmness of the cross-linked structures in polyamide imide was conducted. Pistons having the diameter of 52.4mm and the height of 31mm were prepared and all of them were weighted before coating. This weight is referred to as W_1 . The existing and modified material was screen-printed on the piston skirts respectively followed by curing at 190°C, 200°C or 210°C for 30 minutes in an electrical oven. The typical appearance after curing is shown in Figure 1. Each piston was again weighted here, and this weight is referred to as W_2 representing the weight of the piston with the coating. Subsequently, the pistons were immersed in N-methyl-2-pyrrolidone, which is the solvent for these materials, at ambient temperature for 2 hours followed by heating at 180°C for 60 minutes to dry up the solvent completely. Incomplete cross-linked structures are expected to dissolve out through these processes, resulting a weight loss of the coating. Thus, third weight measurement was carried out after this treatment, and it is referred to as W_3 . The percentage of the resin which did not dissolve during the immersion, R_{rem} , is calculated by Equation (1). This value is considered as an indicator of the firmness of the cross-linked structures. Each test was conducted 3 times.

$$R_{rem} = \left(1 - \frac{W_2 - W_3}{W_2 - W_1} \right) \times 100 [\%] \quad (1)$$

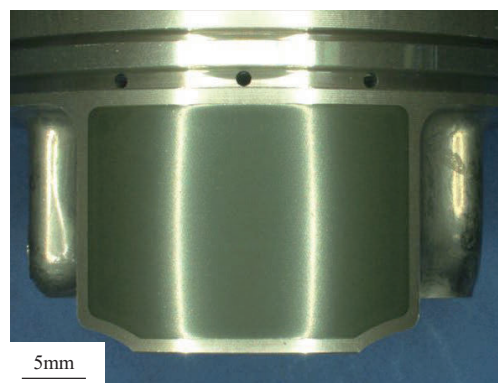


Fig. 1 Appearance of test piston

2-2. Frictional characteristic of new resin

Secondly, frictional characteristics were evaluated by using SRV tester from Optimol Instruments Prüftechnik GmbH. Barrel-shaped test specimens as shown in Figure

2 (a) were prepared from a continuous cast bar used for a forged piston production. This is Al-12wt%Si-4Cu-1Mg alloy including small amount of other alloying elements and given T7 heat treatment. These test specimens were spray-coated with either existing or modified material followed by curing at 200°C for 30 minutes. The coating thicknesses were measured by an eddy current thickness meter, which ensured those of all the test specimens were approximately 15µm. Test specimens whose geometry is described in Figure 2 (b) were also prepared from an actual DiASil cylinder block made of Al-17wt%Si-4.5Cu-0.5Mg alloy including small amount of other alloying elements and given T5 heat treatment. As can be seen from Figure 3, the curved surface remained in a state of the actual cylinder bore where a cross-hatched pattern was induced by a honing process as shown in Figure 4.

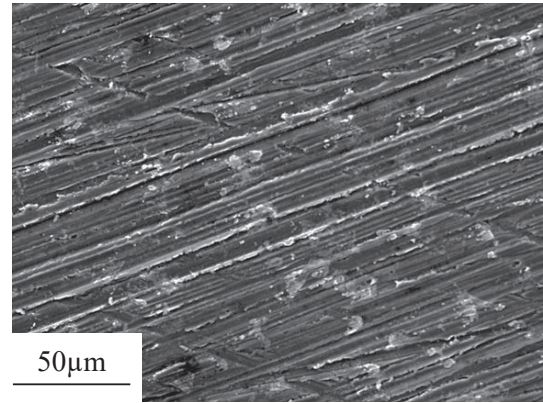


Fig. 4 Morphology of DiASil cylinder bore

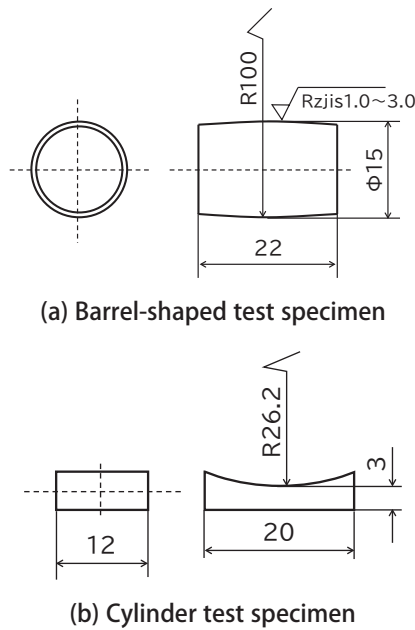


Fig. 2 Geometry of test specimen for SRV test

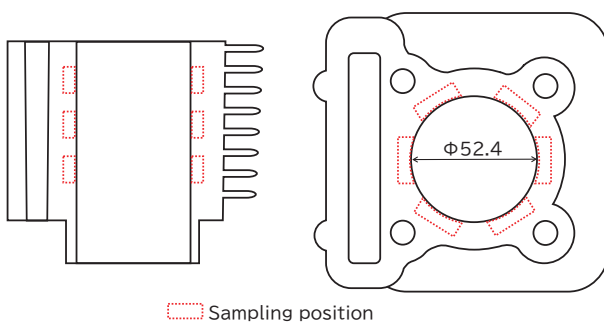


Fig. 3 Sampling position of cylinder test specimen

Figure 5 shows a schematic illustration of SRV tester. The barrel-shaped test specimen and the cylinder test specimen were installed onto the upper and lower specimen holders respectively which were designed to make each test specimen contact at the center of them as described in Figure 6. A normal load was applied through a loading system consisting of a servo motor and a ball screw shown as “load motor” in Figure 5. A horizontal reciprocating motion was provided by a linear motor. The lower specimen holder was filled with oil enough to entirely immerse the contact area between each test specimen. The setting temperature was adjusted so that the contact area could be held at 200°C. During the test, the normal load, horizontal load and friction coefficient were monitored by the equipped sensors. Detailed test conditions are summarized in Table 1. Each test was conducted 3 times.

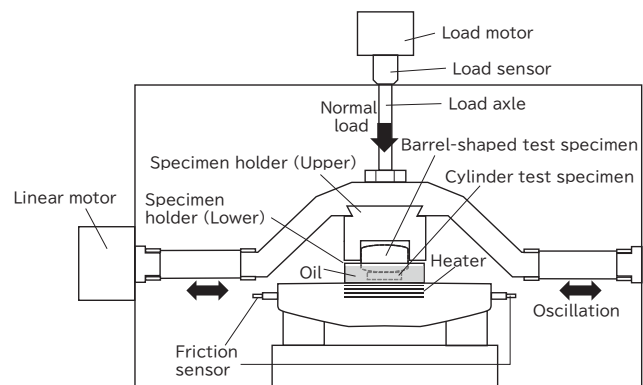


Fig. 5 Schematic illustration of SRV test

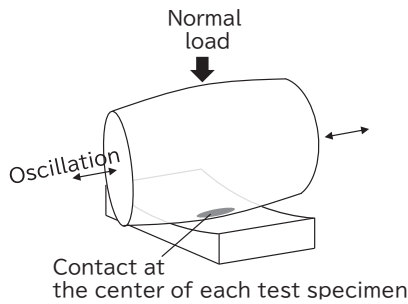


Fig. 6 Contact area between test specimens

Table 1 Detailed condition of SRV test

Normal load	30N
Frequency	10Hz
Stroke	1mm
Oil	SAE 10W-40
Lubrication condition	Immersion
Test duration	1800s

2-3. Wear and seizure characteristic of piston skirt with various surface geometry

Actual pistons having various surface geometries were prepared for this test. The surface geometry in detail is described in the next section. The skirts of the piston were machined according to several conditions before coating. Subsequently, the pistons were screen-printed with the existing material followed by curing at 200°C for 30 minutes. The printing parameters were adjusted so that the grooves on the piston skirts could be filled with the coating material adequately. DiASil cylinder mentioned above was also used for this test and cut into a geometry shown in Figure 7. The curved surface still remained in a honed state as well as the test specimen used in SRV test. A reciprocating slide tester as shown in Figure 8 was used to evaluate wear and seizure characteristics of the pistons with various surface geometries. The piston was attached to the piston holder through the horizontally placed pin. It can rotate around and slide along the pin so that the piston can have self-centering mechanism along with the curvature of the cylinder test specimen. The cylinder test specimen was fixed in the pan in which cartridge heaters were inserted and oil was pooled adequately enough to entirely immerse the sliding interface. The piston holder can be reciprocated by rotation of the crank connected to the

driving motor through the decelerator. The cylinder test specimen was lifted up and pressed against the piston skirt by putting weights on the hanger connected to the pan through the link mechanism. A side view of the reciprocating slide tester is schematically illustrated in Figure 9. The test was stopped at certain intervals to observe a state of the piston skirt surface by an optical microscope and SEM, and then continued until a seizure occurred. The timing of the seizure was detected by an abnormal behavior of the tester such as increasing noise and/or visible oil turbidity (blackening). The detailed test conditions are shown in Table 2.

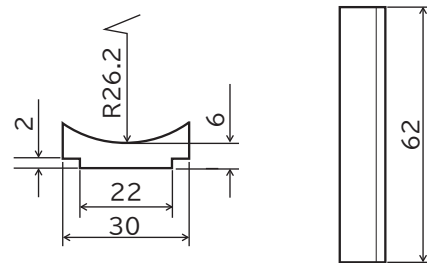


Fig. 7 Geometry of cylinder test specimen

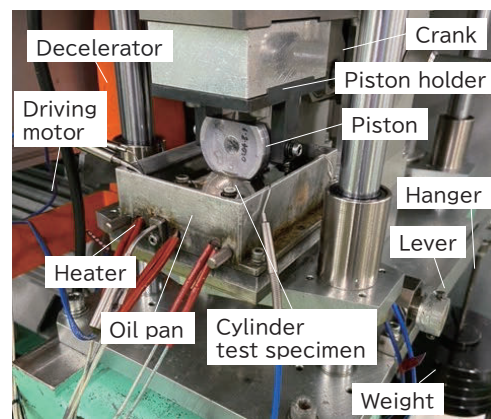


Fig. 8 Reciprocating slide tester

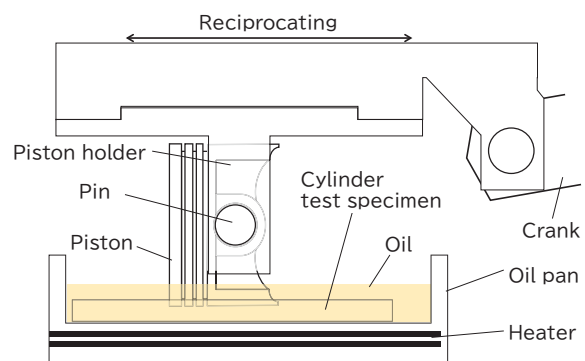


Fig. 9 Schematic illustration of side view

Table 2 Detailed condition of reciprocating slide test

Normal load	100kgf
Crank rotation speed	217rpm
Stroke	20mm
Oil	ISO VG10
Oil temperature	140°C
Lubricant condition	Immersion

2-4. Definition of surface geometry

A geometry of the piston skirt surface is defined by a curvature of a tip of a turning tool (R) and a pitch of a lathe turning (f). The tip of the turning tool is shown in Figure 10. Figure 11 shows a description of a turning process for a piston skirt. The relationship among the surface geometry, R and f is shown in Figure 12. The theoretical surface geometry is determined by following equations.

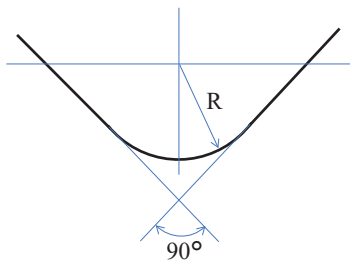


Fig.10 Tip shape of turning tool

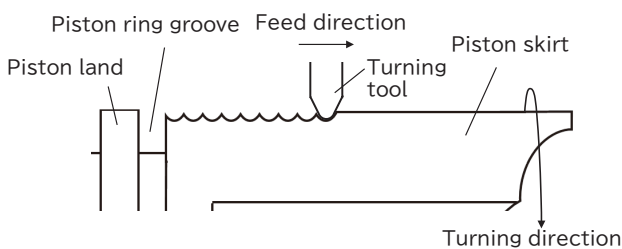


Fig. 11 Description of turning process

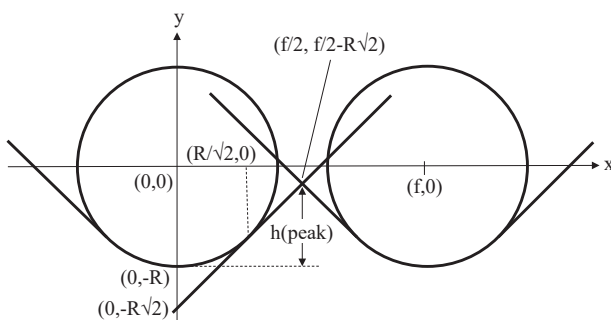


Fig. 12 Surface geometry as function of R and f

In the case of $R / \sqrt{2} \leq f / 2$,

$$h(\text{peak}) = f / 2 + (1 - \sqrt{2})R \tag{2}$$

In the range of $0 \leq x \leq R / \sqrt{2}$,

$$y = -\sqrt{(R^2 - x^2)} \tag{3}$$

$$h = R - \sqrt{(R^2 - x^2)} \tag{4}$$

In the range of $R / \sqrt{2} \leq x \leq f / 2$,

$$y = x - \sqrt{2}R \tag{5}$$

$$h = x + (1 - \sqrt{2})R \tag{6}$$

In both ranges,

$$t_p = (f / 2 - x) / (f / 2) \tag{7}$$

In the case of $0 \leq f / 2 \leq R / \sqrt{2}$,

$$h(\text{peak}) = f / 2 + (1 - \sqrt{2})R \tag{8}$$

$$y = -\sqrt{(R^2 - x^2)} \tag{9}$$

$$h = R - \sqrt{(R^2 - x^2)} \tag{10}$$

$$t_p = (f / 2 - x) / (f / 2) \tag{11}$$

Here,

$h(\text{peak})$: peak height of the geometry

h : height of the geometry

t_p : bearing ratio of Al substrate

A bearing ratio of the Al substrate, t_p , indicates how much percentage the Al substrate accounts for at a certain height as illustrated in Figure 13. Thus, it can be also described by Equation (12).

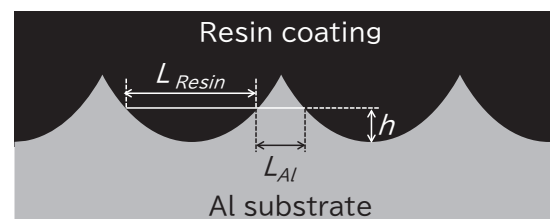


Fig. 13 Parameter description for bearing ratio

$$t_p = L_{Al} / (L_{Al} + L_{Resin}) \tag{12}$$

In this paper, the several surface geometries on the piston skirt were prepared with changing the values of R and f as shown in Table 3. Figure 14 shows theoretical geometries of various specifications.

Table 3 Parameter for each surface geometry

	R / mm	f / mm
Rz2Sm150	1.50	0.15
Rz12Sm100	0.10	0.10
Rz18Sm120	0.10	0.12
Rz18Sm260	0.46	0.26
Rz25Sm140	0.10	0.14

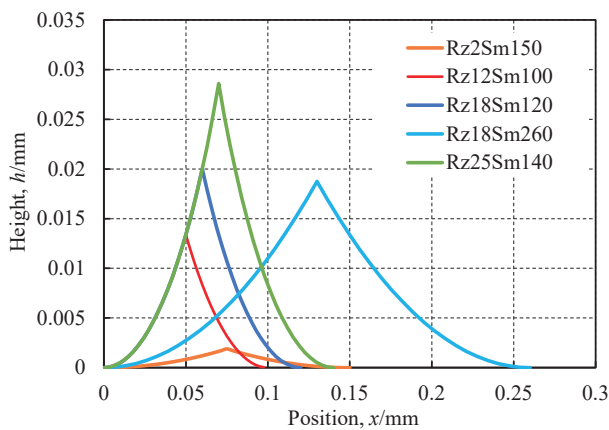


Fig. 14 Theoretical surface geometry

3 RESULTS AND DISCUSSION

3-1. Characteristic of developed coating

The percentages of undissolved resin, R_{rem} , based on Equation (1) are presented in Figure 15. Each bar chart shows the average value of the 3 measurement results. R_{rem} of the existing material increased as the curing temperature raises. However, there is a significant divergence from complete firmness even cured at 210°C. The modified material had the higher value compared to the existing material under any curing conditions and it reached 100% by curing at 200°C and 210°C. This result suggests the modified material is easily encouraged to form the strong cross-linked structures even at a relatively low temperature.

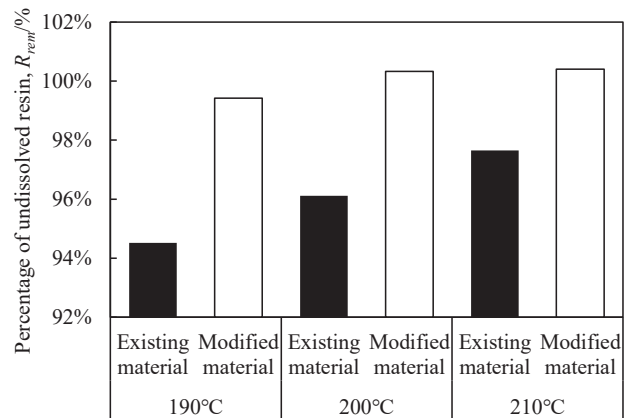
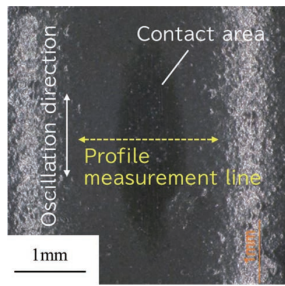
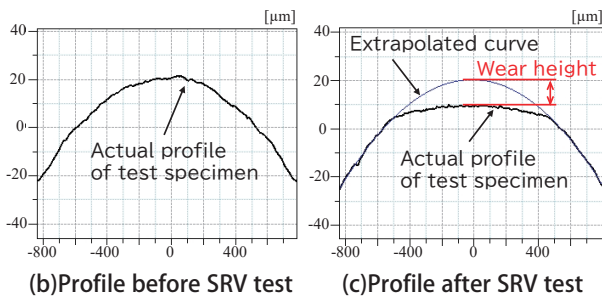


Fig. 15 Percentage of undissolved resin

Figure 16 shows a typical appearance of the barrel-shaped test specimen after SRV test and profiles before and after the test measured by a contact profilometer. The wear height, h_{wear} , was defined as a gap between a profile before the test and the one after the test. For measurement of wear height, a curve extrapolated from a profile of non-contact area was used instead of an actually measured profile as an initial shape of the test specimen since it was challenging to completely match the measurement points before and after the test. The average wear heights of each material are shown in Figure 17. The value of modified material was around 25% lower than that of the existing material. The change in the friction coefficient, μ , during the test is shown in Figure 18. The friction coefficient of the modified material seems to be more stable than that of the existing material. A polyamide imide takes on a role of holding the additives such as solid lubricants and hard fillers. The modified polyamide imide may prevent these additives from dropping out easily and enable these additives to fully exert their functions during sliding. From these results, it can be considered the increase of the strong cross-linked structure in the resin coating could improve not only wear resistance but also friction coefficient stability.



(a) Appearance after SRV test



(b) Profile before SRV test (c) Profile after SRV test

Fig. 16 Typical appearance and profile of barrel-shaped test specimen and definition of wear height

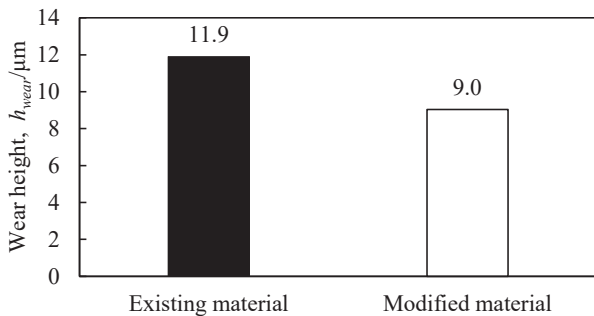


Fig. 17 Wear height after SRV test

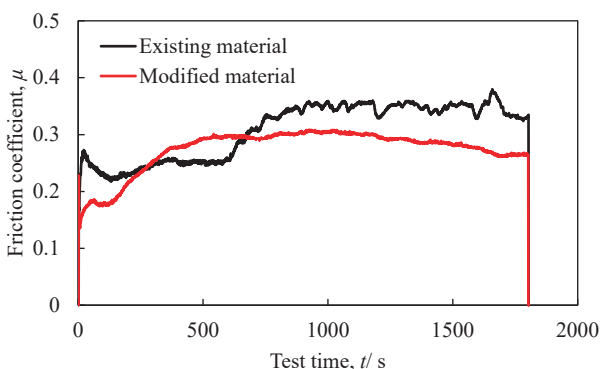


Fig. 18 Friction coefficient during SRV test

3-2. Comparison of piston surface geometry between theoretical and experimental result

The surface roughness parameters, Rz_{jis} and Sm , of the piston skirts after machined (before coating) under the

conditions listed in Table 3 were measured at the center of the skirt along the piston height direction as presented in Table 4. The representative of actually measured bearing curves is described with theoretical one derived from Equation (2)-(11) in Figure 19. It is found the experimentally measured curve shows a good agreement with the theoretical curve.

Table 4 Measurement result of surface roughness

	Experimental result	
	$Rz_{jis} / \mu m$	$Sm / \mu m$
Rz2Sm150	1.5	120.6
Rz12Sm100	11.9	100.1
Rz18Sm120	19.1	120.4
Rz18Sm260	19.1	260.1
Rz25Sm140	25.2	140.2

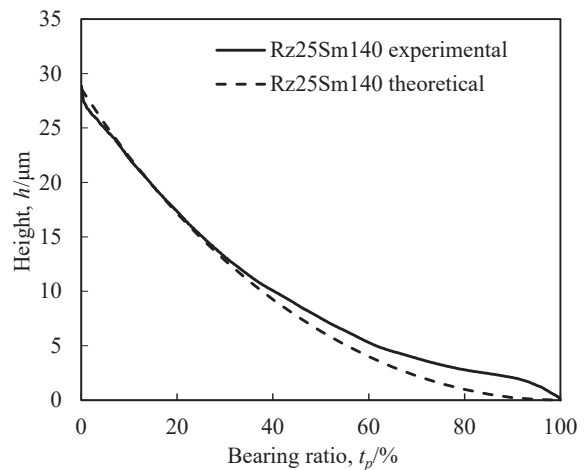


Fig. 19 Comparison between theoretical and experimental bearing curve

3-3. Effect of piston skirt surface geometry on wear and seizure property

The effect of the piston skirt geometry on the wear and seizure property was investigated using the reciprocating slide tester. A typical morphological transition of the skirt surface during the test is shown in Figure 20 obtained from Rz18Sm120 specimen. The pictures in left side are secondary electron image micrographs and the right ones present carbon distribution analyzed by an energy dispersive X-ray spectroscopy. Comparing these pairs, it can be seen that there is a striped pattern consisting of the Al substrate and the resin coating. Prior to this evaluation, each piston skirt surface was initially run in

until the Al substrate was slightly exposed to the sliding surface. Therefore, the Al substrate could be preliminarily observed at the beginning of the test (0 second). In addition, this pretreatment served to smoothen and conform the surface roughness among the various surface specifications. As the wear of the piston skirt surface proceeded, the area of the Al substrate gradually spread in the sliding direction while that of the resin coating complementarily diminished, finally leading a seizure at 9900 seconds as shown Figure 21. It is worth noting that the seizure did not take place until 9900 seconds even though the Al substrate was already exposed to the sliding interface in the early stages. Similar phenomena were found in the tests of the other skirt surface geometries.

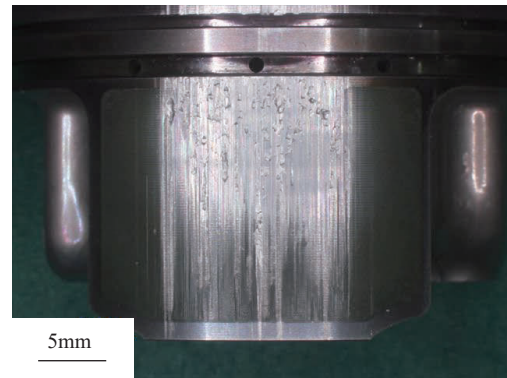


Fig. 21 Appearance of seizure at 9900 seconds

According to Equation (12), the bearing ratios of the exposed Al substrate of each piston skirt surface were measured by an image analysis of the SEI micrographs, and the value was used as an indicator of the wear of the piston skirt geometry. That is to say, the bearing ratio of the Al substrate reaching 100% indicates the grooves accommodating resin coating have been worn out and the surface has consisted of the only Al substrate. The relationships between the bearing ratio of the Al substrate of each piston skirt geometry and the test time are shown in Figure 22. As mentioned above, each piston skirt surface was run in until the Al substrate was slightly exposed to the sliding surface in advance. Therefore, the each bearing ratio of the Al substrate had different values at the beginning of the test (0 second). As can be seen from Figure 22, there seems to be proportional relationships between the bearing ratio of the Al substrate and the test time in every case. Additionally, the slopes of those, meaning an exposure rate of the Al substrate, seemingly become smaller with increasing the skirt roughness. The seizure occurrence moments of each piston are shown in Figure 22 as color-coded dotted lines. Thus, intersections of the solid lines with the dotted lines indicate estimated bearing ratios of the Al substrate when the seizure occurred as plotted by the asterisks in the graph. From this result, it is clear the deeper grooves on the piston skirts can play an effective role to delay the seizure. The additional point to be noted in this graph is that all the seizures were triggered when the bearing ratio of the Al substrate reached up to 60-80% as described by horizontal red lines, implying the bearing ratio of the Al substrate can be the empirical criteria for the seizure.

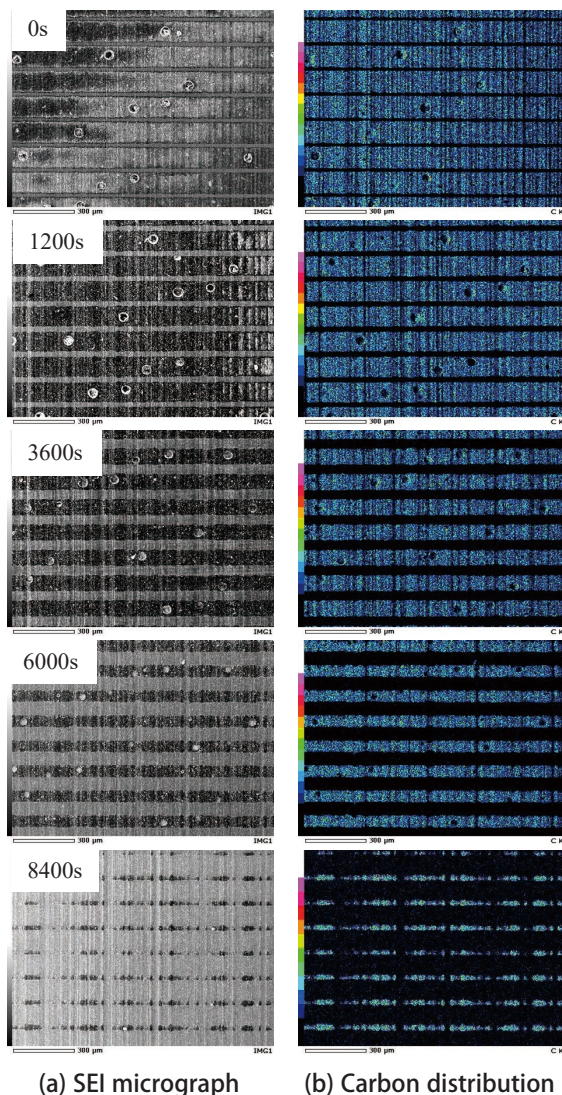


Fig. 20 Typical morphology transition of skirt surface

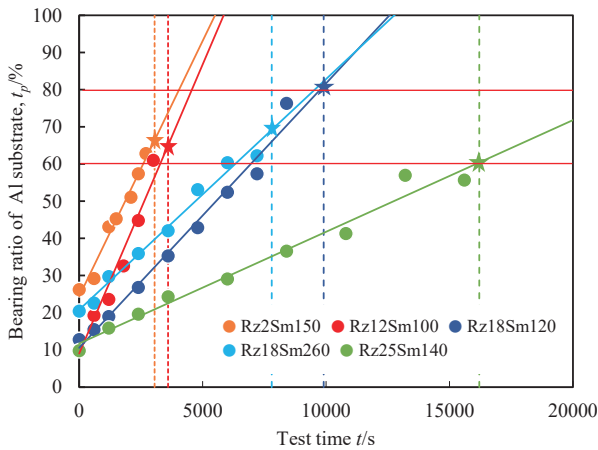


Fig. 22 Bearing ratio of Al substrate as function of test time

3-4. Influential factor for seizure

Somi *et al.* investigated seizure resistance of binary Al-Si alloys and found wear types transitioned from mild wear to seizure with increasing a load^[5], which implies a stress can be one of the influential factors for the seizure. Thus, the stress distribution was calculated by a contact analysis software, TED/CPA version 854 made by TriboLogics Corporation. Physical properties used for the calculation are listed in Table 5. A mating material is Al having flat surface. Nominal pressure between the surfaces was 100MPa.

Table 5 Physical properties used for analysis

	Al substrate	Resin
Elastic modulus, E/Gpa	77.8	4.0
Poisson's ratio	0.37	0.43

A typical calculation result is shown in Figure 23. Stress concentrations are observed at the edges of the Al substrate contact surface. On the other hand, the stress on the resin portion is much lower than that on the Al portion. In order to investigate the change in the stress on the Al and resin portions with increasing the bearing ratio of Al substrate, the highest values as the stress working on Al and the lowest values as the stress working on resin are picked up from the calculation results, then plotted these values against the bearing ratio of the Al substrate as shown in Figure 24. Considering the origin of the seizure, maximum pressure induced to

the Al substrate should be noted rather than that on the resin coating since the seizure will occur from a metal-to-metal contact. Then, it is found the maximum pressure on the Al substrate becomes smaller as the bearing ratio of the Al substrate increases. Therefore, the hypothesis of the stress-induced seizure cannot explain the phenomena observed in this study.

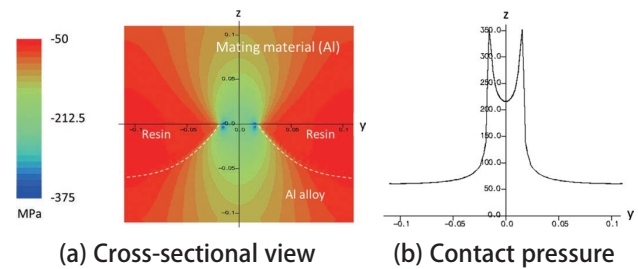


Fig. 23 Contact pressure distribution

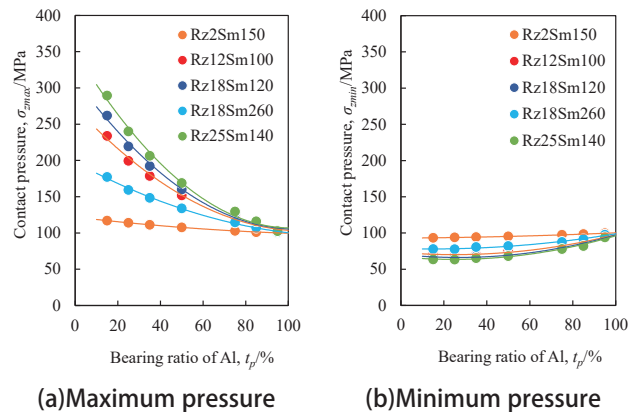


Fig. 24 Change in contact pressure with increasing bearing ratio of Al

It was implied above that the bearing ratio of the Al substrate could be the empirical criteria for the seizure, which indicates the coating remained in grooves may play a key role to prevent the seizure. To verify an effect of it on the seizure, a non-coated piston with Rz18Sm100 was additionally tested. The load during running in was lowered to one-tenth of the previous test, namely 10kgf, so that the seizure could not be triggered. After confirming by SEM observation that the tips of the grooves were slightly worn and flattened as shown in Figure 25, a main test was conducted under the conditions in Table 2. As the result, a seizure was observed within only 120 seconds after the main test started as shown in Figure 26, which demonstrably

proved the coating in the grooves could serve to prevent the seizure.

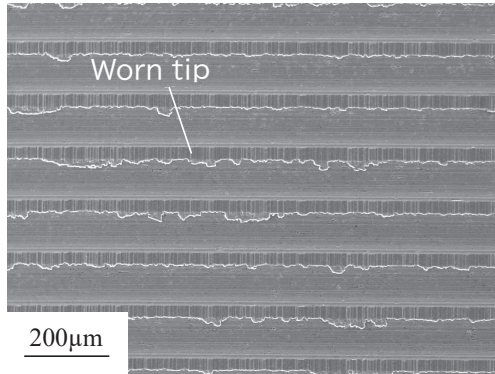


Fig. 25 Morphology of skirt surface after running in

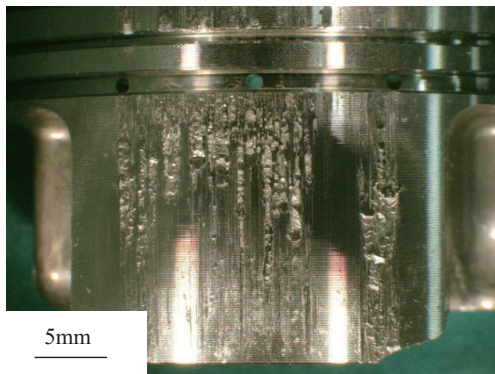


Fig. 26 Appearance of seizure at 120 seconds

A conceivable mechanism of the seizure prevention by the resin coating in the grooves is schematically described in Figure 27. As can be seen in this figure, the worn resin coating is sure to pass over the surface of the adjacent Al substrate since the piston was reciprocated in the direction perpendicular to the grooves. The resin coating transferred to the Al substrate could cover the exposed Al substrate and deter the metal-to-metal contact, resulting in the prevention of the seizure. In the early stage of the Al substrate exposure, deep grooves could keep the adequate resin coating enough to protect the adjacent Al substrate entirely. However, amount of the resin coating stored in the grooves would gradually decrease with the progress of the wear in the latter stage. In addition, the Al substrate to be protected would increase contrarily. Thus, the seizure could finally happen from a part of the Al substrate not covered with the resin coating. Further investigations and considerations are still

required to verify this hypothetical mechanism. For example, surface composition analyses of the piston and the cylinder test specimen during the test would enable us to confirm whether the worn and transferred resin coating actually covers the Al substrate.

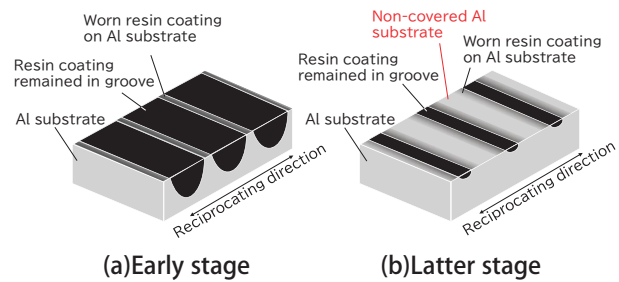


Fig. 27 Conceivable mechanism of seizure prevention by resin coating in groove

3-5. Printability of deep groove

As mentioned above, the seizure can be delayed with the deeper grooves on the piston skirts. However, it is expected deeper grooves would show larger roughness even after coating, which is one of concerns about an increase in the friction loss as reported in the previous studies^{[6][7]} especially at the early stage of an engine operation. Thus, the roughness after coating with the different surface geometries was evaluated. The pistons were screen-printed under the condition individually optimized for each geometry. Through this process, grooves of each geometry were covered and filled with the resin coating material. The roughness, Rz_{jis} , on the piston skirt covered with the resin coating was measured at the center of the skirt along the piston height direction. After coating, all the pistons except the one with $Rz2Sm150$ showed smaller roughness than as-machined state owing to the leveling effect as shown in Figure 28. In case of $Rz12Sm100$ and $Rz18Sm120$, the roughness after coating were comparable to that of $Rz2Sm150$. On the other hand, substantially large roughness still remained in case of the pistons with $Rz18Sm260$ and $Rz25Sm140$. It had been confirmed the roughness could be further reduced by using a multiple screen-printing technique, but it will also lead an increase in the process flow resulting in a cost increase. Thus, in practical use, it is necessary to choose a suitable geometry with considering required durability, surface roughness and cost.

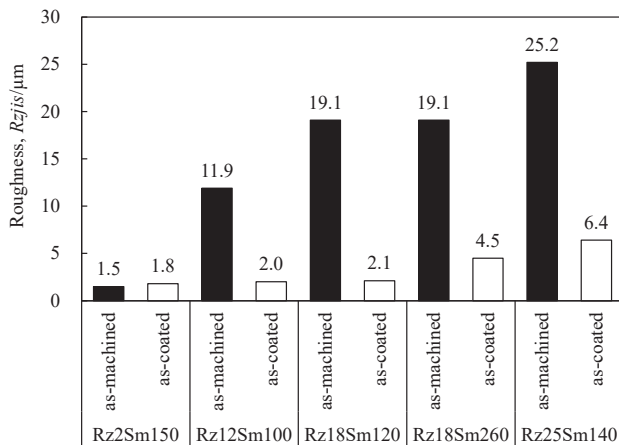


Fig. 28 Roughness before/after coating

4 CONCLUSION

In this research, the effects of the modified resin coating and the deep grooves on durability of the resin coated piston were investigated, and which has led following conclusions.

- (1) The polyamide imide was modified so that it can be cured completely at a relatively low temperature. As the result, frictional characteristics were improved compared to the existing coating.
- (2) It was found the deeper grooves on the piston skirts can play an effective role to delay the seizure.
- (3) Seizures were triggered when the ratio of the Al substrate exposed to the sliding surface reached up to 60-80%, which implies the coating remained in grooves may play a key role to prevent the seizure.
- (4) Roughness on the piston skirt was reduced after the coating process owing to the leveling effect. The deeper grooves tended to remain relatively large roughness even after coating.

ACKNOWLEDGEMENT

The authors would like to acknowledge Dr. Kunihiko Kakoi of TriboLogics Corporation for his dedicated cooperation for the contact analysis.

REFERENCES

- [1] K. Holmberg, P. Andersson and A. Erdemir, "Global energy consumption due to friction in passenger cars," *Tribology International* 47, (2012), 221-234.
- [2] H. Kurita, H. Yamagata, H. Arai and T. Nakamura, "Hypereutectic Al-20%Si alloy engine block using high-pressure die-casting," SAE Technical Paper 2004-01-1028, (2004).
- [3] T. Uhara and H. Kurita, "The Effect of Surface Morphology of Cylinder Bore Surface on Anti-Scuffing Property made by High Pressure Die-Casting Process using Hyper-Eutectic Al-Si Alloy," *SAE Int. J. Mater. Manf.* 7(1), (2014). doi:10.4271/2013-32-9046
- [4] K. Watanabe, T. Sato, T. Aoki, F. Ito *et al.*, "Development of Piston Resin Coating suitable for DiASil Cylinders," *Yamaha Motor Technical Review*, (2018), 76-81.
- [5] A. Somi Reddy, B. N. Pramila Bai, K. S. S. Murthy and S. K. Biswas, "Wear and seizure of binary Al-Si alloys," *Wear* 171, (1994), 115-127.
- [6] M. Takiguchi, T. Takimoto, E. Asakawa, K. Nakayama *et al.*, "A Study of Friction Force Reduction on Piston Skirt (Effect of Width, Roughness and Resin Coating)," *Transaction of the JSME* 63(611), (1997), 327-332.
- [7] M. Sasaki, N. Takahashi, T. Sato and S. Sue, "Development of Low Friction Solid Film Lubricant for Piston (1) Development of Double Layer Solid Film Lubricant," 2010 JSAE Spring Convention Proceeding, (2010), 7-10.

■ 著者



渡邊 慧太
Keita Watanabe
生産技術本部
材料技術部



栗田 洋敬
Hiroataka Kurita
生産技術本部
材料技術部